Evaluating Bicarbonate Electrolyzer Configurations for EnergyEfficient Formate Production

ADVANCED SUSTAINABLE SYSTEMS
www.advsustainsys.com

Evaluating Bicarbonate Electrolyzer Configurations for Energy-Efficient Formate Production

Alessio Mezza, Juqin Zeng, Marco Etzi, Daniele Sassone, Fabrizio C. Pirri, and Adriano Sacco**

Reactive carbon capture (RCC) by direct conversion of CO_2 capture solutions has emerged as a promising alternative to gas-fed electrolyzers. Leveraging bicarbonate electrolyzers (BEs), RCC eliminates energy-intensive steps such as CO_2 regeneration and pressurization. Additionally, BEs prevent failures like carbonate salt deposition common in gas-fed systems. However, intrinsic challenges in BEs, such as higher cell voltages and lower faradaic efficiencies (FEs), result in greater energy consumption during electrolysis compared to gas-fed electrolyzers. To evaluate whether an RCC chain (RCCC) is more energy-efficient for formate production than a gas-fed carbon chain (GFCC), the study optimizes the BE configuration and compares it to a valorization chain requiring a pure, pressurized CO_2 stream for gas-fed electrolyzers. This study shows the most efficient BE setup employs a cation exchange membrane paired with a buffer layer, achieving a FE for formate of ≈75% at a current density of 100 mA cm^{-2} and a cell potential of 3.1 V. Using this optimized BE, the RCCC demonstrates an energetic advantage over GFCCs in scenarios without CO_2 recycling. Even with 100% CO_2 utilization enabled by recycling systems, RCCC remains competitive. With potential improvements in BE performance, RCCC emerges as a promising strategy for converting CO_2 into formate efficiently.

1. Introduction

Over the past few decades, human activities have significantly increased atmospheric CO_2 levels, prompting the scientific community to develop technologies aimed at reducing reliance on fossil fuels. While the transition to renewable energy is progressing, it remains a gradual process, making it essential to minimize carbon emissions during this period. In this context, the electrochemical reduction of CO_2 (eCO_2RR), powered by renewable energy, has emerged as a promising solution.[1] This process enables the conversion of CO_2 into valuable chemicals and fuels, offering a pathway to a more sustainable and circular carbon economy.[1,2] Among the different products obtainable through the electroreduction of CO_2, formic acid (HCOOH) and its derivative, formate ($HCOO^-$), hold significant potential as energy carriers in fuel cell technologies, as well as building block for the chemical industry.[3]

Recently, gas-fed CO_2 electrolyzers, which operate by directly delivering CO_2 in its gaseous form, have attracted considerable attention. By delivering CO_2 in stoichiometric excess, these systems achieve high Faradaic efficiency (FE > 90%) even at elevated current densities (>300 mA cm^{-2}).[4] However, gas-fed electrolyzers face challenges, including low carbon efficiency and operational instability caused by salt deposition.[5] One approach for utilizing gas-fed electrolyzers involves establishing a carbon value chain, as illustrated in **Figure 1**. This process begins with an alkaline-based capture method that efficiently extracts CO_2 from industrial flue gas or the atmosphere. Once captured, the CO_2 is regenerated and delivered to the electrolyzer. However, the regeneration and compression of CO_2 from the capture solution require significant energy input, which poses a challenge to the overall efficiency of the system.[6] Moreover, modern membrane electrode assembly (MEA) gas-fed alkaline electrolyzers are unsuitable for CO_2 electro-reduction into formic acid/formate.[7] In fact, while these systems are characterized by high FEs and current densities for gaseous eCO_2RR products like CO, the use of anion exchange membranes (AEMs) leads to the crossover of $HCOO^-$ anions toward the anode, where they are re-oxidized, releasing CO_2 and H_2O, thus rendering the CO_2 conversion ineffective.[7] To address this, recent developments in three-chamber gas-fed reactors have emerged as a possible solution. By combining cation exchange membranes (CEMs) and AEMs, these reactors enable formic acid production in the

A. Mezza, J. Zeng, F. C. Pirri
Department of Applied Science and Technology
Politecnico di Torino
Corso Duca degli Abruzzi 24, Torino 10129, Italy
E-mail: alessio.mezza@polito.it

A. Mezza, J. Zeng, M. Etzi, D. Sassone, F. C. Pirri, A. Sacco
Center for Sustainable Future Technologies @Polito
Istituto Italiano di Tecnologia
Via Livorno 60, Torino 10144, Italy
E-mail: adriano.sacco@iit.it

The ORCID identification number(s) for the author(s) of this article can be found under https://doi.org/10.1002/adsu.202500098

DOI: 10.1002/adsu.202500098

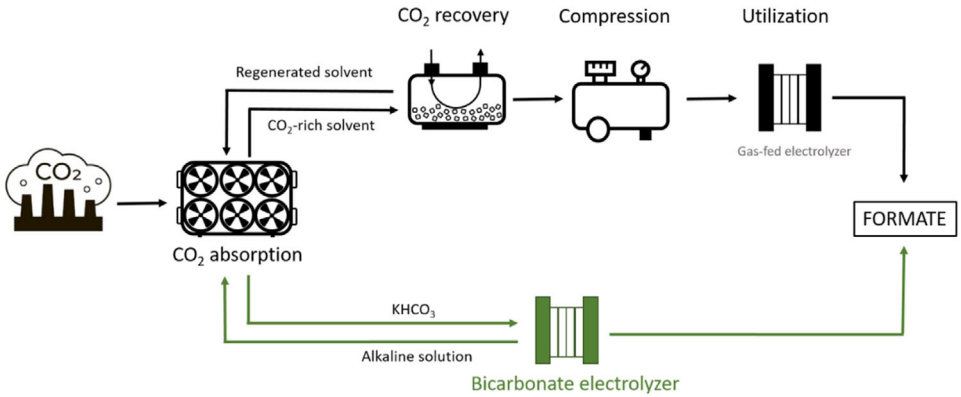

Figure 1. Schematic representation of carbon valorization pathways utilizing electrochemical CO_2 reduction for formate production. The upper pathway illustrates the gas-fed carbon chain (GFCC), while the lower pathway depicts the reactive carbon capture chain (RCCC).

central compartment.[8] This configuration maintains good CO_2-to-HCOOH conversion efficiency, but the inclusion of an additional chamber and membrane increases the cell voltage, which negatively impacts energy efficiency.[8,9]

An alternative to the traditional carbon value chain is offered by reactive carbon capture (RCC) technology, which enables the direct conversion of captured CO_2 into valuable products (Figure 1), eliminating the need for intermediate CO_2 regeneration and compression.[10] In bicarbonate electrolyzers (BEs), CO_2 is generated in situ (i-CO_2) from an aqueous solution of carbonate or bicarbonate due to the acidic region formed on the cathodic side of a bipolar membrane (BPM) under reverse bias (**Figure 2**) in a zero-gap MEA reactor.[10a,b] The i-CO_2 is then electro-reduced to formic acid in the form of formate, owing to the neutral pH of the bicarbonate solution.[11] T. Li et al.[10e] were the first to demonstrate that a BE can convert CO_2 into formate using a liquid feedstock. BPMs allow independent operation of the cathode and anode sides. They generate H^+ and OH^- at the cathode and anode, respectively, as a result of water splitting between the BPM layers.[12] The use of a BPM enhances anodic catalysis, enabling stable operation with a cost-effective Ni-based electrode in alkaline solution, as the continuous regeneration of OH^- compensates for its consumption.[13] By employing reactive carbon capture, a simplified carbon value chain for potential pilot-scale plants (Figure 1) becomes possible. Although the RCC approach eliminates the need for separate CO_2 regeneration and compression, the use of BPMs results in a high cell voltage, which increases the energy consumption per mole of formate produced.[14] Zhang et al.[15] proposed a potential solution by employing the hydrogen oxidation reaction (HOR) in place of the oxygen evolution reaction (OER) to lower the cell voltage. However, this approach needs a high value reagent like

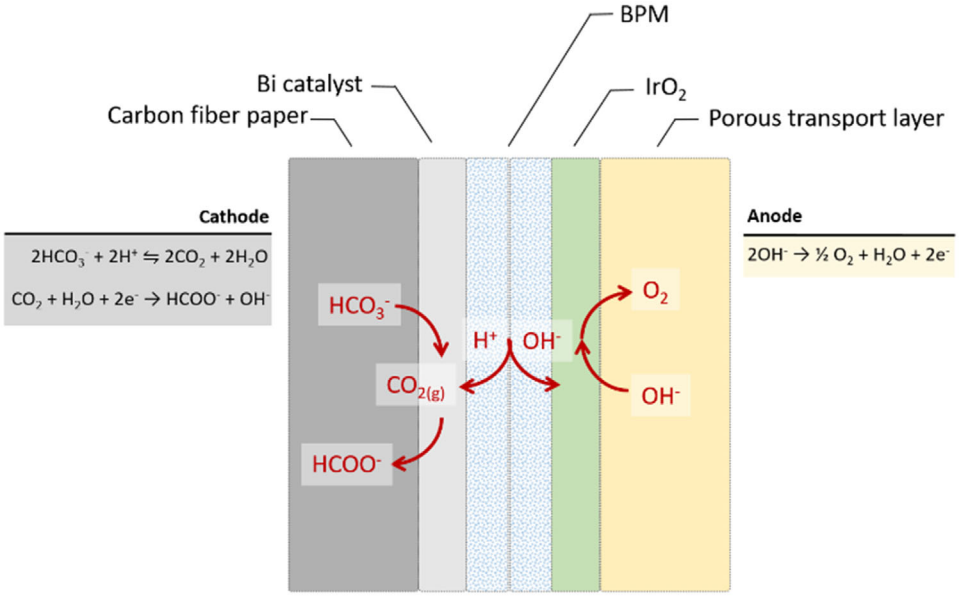

Figure 2. Schematic depiction of the chemical and electrochemical reactions taking place in the bicarbonate electrolyzer, highlighting the processes occurring at the anode and cathode.

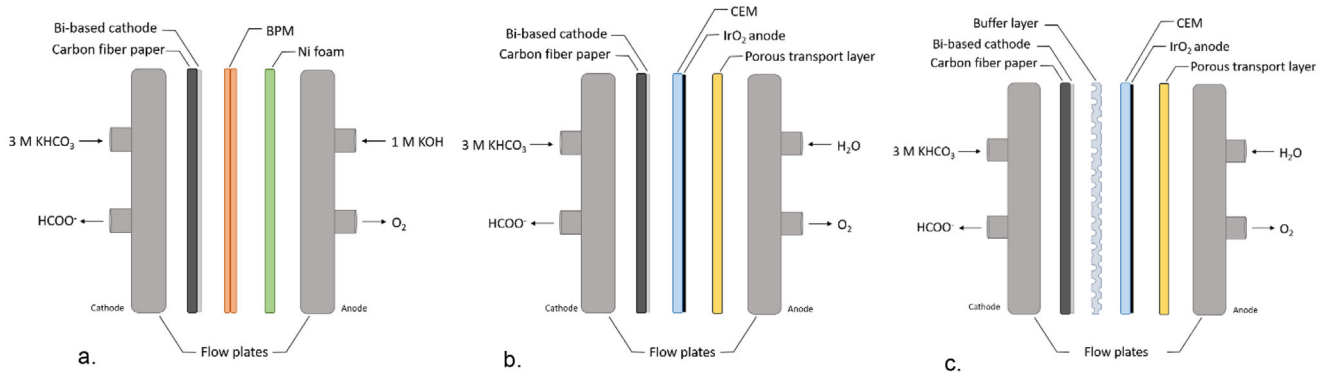

Figure 3. Schematic overview of the bicarbonate electrolyzer configurations examined. All setups utilize a bismuth-based catalyst for CO_2RR: a) **BPM**: Incorporates a bipolar membrane in reverse bias with a Ni foam anode. b) **CEM**: Employs a cation exchange membrane coated with IrO_2 as the anodic catalyst and a Pt-Ti felt as the transport layer. c) **CEM-BL**: Features a porous buffer layer, consisting of a mixed cellulose ester filter membrane, positioned between the CEM and the cathode.

hydrogen, raising the cost of this technology. Recently, CEMs are being considered as promising alternatives to BPM to create an acidic region necessary to release CO_2. CEM configuration delivers protons to the cathode using an acidic solution or pure water as anolyte, thus requiring more expensive Ir-based electrode as anode. CEMs partially reduced the cell voltage but it also resulted in reduced eCO_2RR efficiency: Faradaic efficiency in BEs is typically below 70% at industrial-level current densities.[13] Lee et al.[16] were the first to use a CEM in a standard BE to produce multicarbon products from (bi)carbonate. In order to achieve high FEs, they employed a buffer layer (BL) interposed between the CEM and the CO_2RR catalyst. A hydrophilic porous material used as buffer layer lets HCO_3^- species to diffuse toward the CEM that provides H^+. Therefore, in proximity of the CEM, *i*-CO_2 is released from (bi)carbonate due to the low local pH. Recovered CO_2 diffuses through the buffer layer toward the Bi-catalyst, where CO_2RR occurs farther from the acid region created by the CEM. This implies that a highly porous material must be used as a buffer layer. However, its employment increases again the cell voltage. These factors contribute to higher energy consumption per mole of formate produced by BEs. Zhang et al.[11] and Nomoto et al.[17] achieved respectively high carbon efficiency and FEs in CO_2-to-$HCOO^-$ conversion using BEs equipped with a CEM and a buffer layer. While the first one used Sn nanoparticles as CO_2RR catalyst, the second one electrodeposited a Bi catalyst starting from a solution of $Bi(NO_3)_3$. Thus, while research has explored both BPM and CEM alternatives,[16] it is now essential to identify which configuration is energetically more competitive with the gas-fed electrolyzer.

To address this point, in this work, electrolyzer configurations have been compared in terms of their energy efficiency for the CO_2-to-$HCOO^-$ conversion using a bismuth oxide catalyst. To evaluate whether the reactive carbon capture chain (RCCC) is more energy-efficient than the gas-fed carbon chain (GFCC) for the production of formate or formic acid, we focus on key performance metrics including FE, cell voltage, and carbon efficiency for each BE's configuration under consideration, reported in **Figure 3**. Establishing this comparison will help build a solid foundation for advancing this emerging BE technology.

Our results highlight how advancements in bicarbonate electrolyzer designs have enabled the development of RCCC systems that are competitive with GFCCs in terms of energy efficiency.

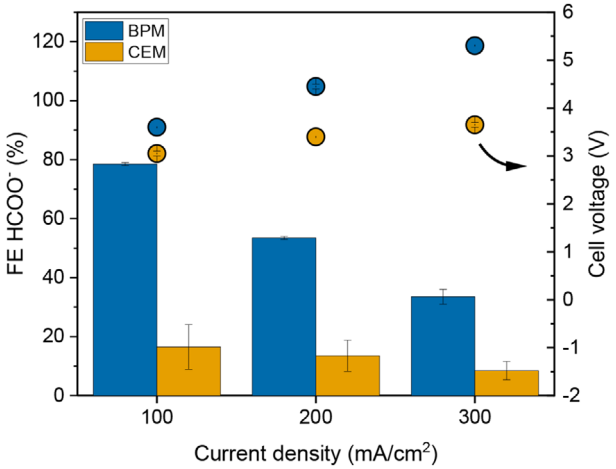

Figure 4. FEs (bars, left axis) and cell voltage (points, right axis) obtained with BPM and CEM configurations.

2. Results and Discussion

2.1. BPM and CEM Configurations

In this work, BPM and CEM configurations for formate electroproduction have been evaluated using a home-made Bi-based catalyst. Particularly, bismuth oxide was synthesized using a microwave-assisted method (see Figure S1, Supporting Information). The obtained catalyst was deposited onto carbon fiber paper via spray coating at a loading of 3 mg cm^{-2} (see Supporting Information). A 3 M $KHCO_3$ solution was delivered to the cathode, where *i*-CO_2 reacts with the catalyst to produce $HCOO^-$. In the BPM BE, 1 M KOH was supplied to the anode, enabling the OER to occur on Ni foam (Figure 3a). In contrast, the CEM configuration utilized an Ir-based electrode that facilitates O_2 generation by

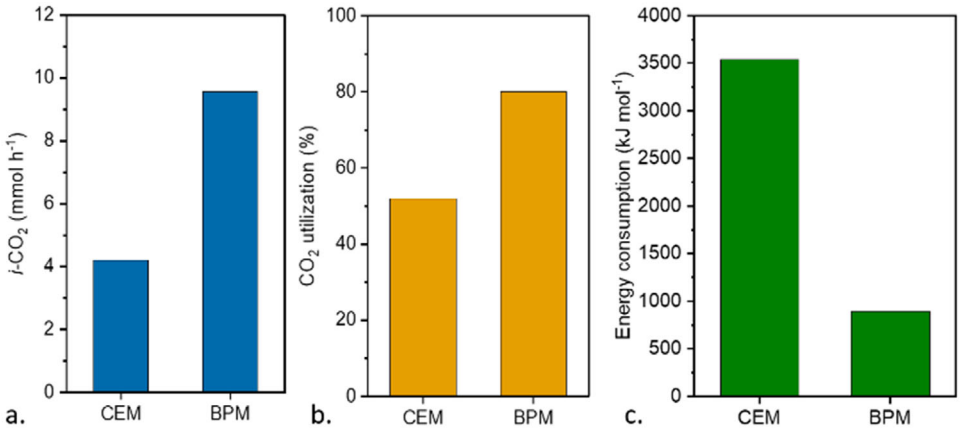

Figure 5. a) In situ recovered CO_2 (i-CO_2), b) CO_2 utilization, and c) and energy consumption per mole of $HCOO^-$ produced (see Supporting Information) by CEM and BPM configurations at 100 mA cm^{-2}.

oxidizing pure H_2O. IrO_2 was deposited on a Nafion N117 membrane through spray coating to create a catalyst-coated membrane (CCM), minimizing voltage losses caused by imperfect interfaces in the MEA (see Supporting Information). A platinized-titanium felt served as the porous transport layer, optimizing liquid-gas diffusion (Figure 3b). In **Figure 4**, cell voltage and FE for formate are shown at current densities ranging from 100 to 300 mA cm^{-2}. In both configurations, FEs for formate decrease with increasing current densities due to excessive acidity caused by the protons delivered by the IEM.[11] The BPM configuration achieves higher FEs, nearing 80% at 100 mA cm^{-2}, but it exhibits significantly higher cell voltages compared to typical values observed in CO_2RR electrolyzers.

Selectivity for CO was negligible as highlighted by Figure S4 (Supporting Information). Typically, gas-fed alkaline electrolyzers maintain cell potentials below 4 V even at 300 mA cm^{-2}.[5b] The elevated cell voltage shown in Figure 4, an intrinsic characteristic of the BPM arising from its sandwich structure of cation and anion exchange layers where water splitting occurs,[18] significantly impacts the energy consumption of formate production. To mitigate this, a CEM can be utilized. As reported in Figure 4, the potential is significantly decreased from 5.3 to 3.6 V at 300 mA cm^{-2}. However, the formate selectivity is severely impacted by the use of the CEM.

From **Figure 5**a, it can be inferred that at the catalyst-CEM interface, a greater fraction of protons delivered from the anode is consumed in HER rather than reacting with HCO_3^-. As a result, the amount of *i*-CO_2 regenerated from (bi)carbonate is substantially lower compared to the BPM configuration. Figure 5b demonstrates that the proportion of CO_2 regenerated and subsequently converted into $HCOO^-$ is reduced from 80% to 52% when a CEM is utilized. Although the cell potential is significantly lower, the reduced FEs make the CEM configuration notably more energy-intensive than the BPM (Figure 5c).

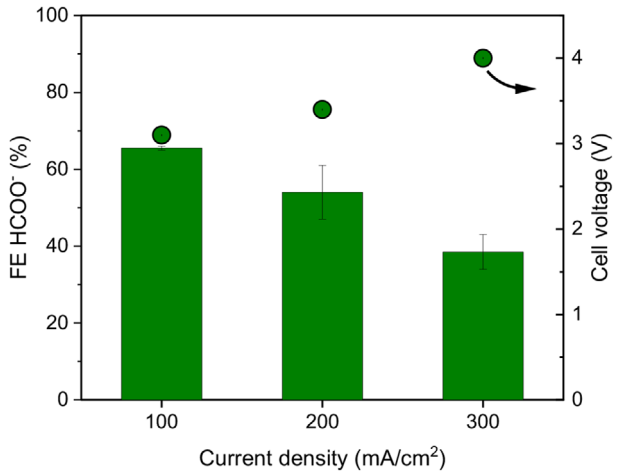

Figure 6. FEs and cell voltages obtained at different current densities with CEM-BL configuration.

2.2. CEM-BL Configuration

Cell potential drop obtained with CEM is a mandatory result that must be pursued to scale up BE technology. In order to recover the FEs for formate, while maintaining such low voltage allowed by CEM employment, a novel approach has recently been proposed. This involves placing a porous buffer layer between the CEM and the cathode.[16] The BL creates a buffer region where H^+ is more likely to react with HCO_3^- to generate in situ CO_2, rather than reaching the cathode and promoting competitive HER. As a result, recovered CO_2 diffuses toward the Bi-catalyst that is positioned farther from the CEM, allowing it to perform CO_2RR in a less acidic environment (Figure 3c). Different porous materials have been used as BL, such as Polyvinylidenefluoride, polyethersulfone, and mixed cellulose esters (MCE) membranes.[16] Recent studies have shown that a commercial MCE membrane with 8 μm pores is suitable for use as a BL in BE. [17] As shown in **Figure 6**, the use of a MCE membrane as a buffer layer restores the formate FE to 66% at 100 mA cm^{-2}, compared to 17% for the CEM without any BL. This is a great result considering the target 80% FE obtained with the BPM; thus confirming the validity of this strategy. The cell voltage in the CEM-BL configuration remains similar to that of

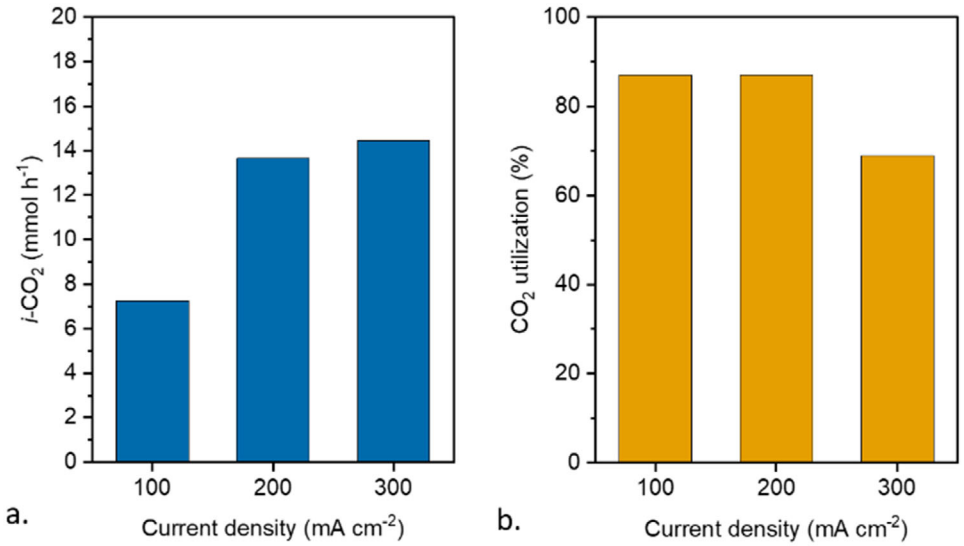

Figure 7. a.) In situ recovered CO_2 (*i*-CO_2) and b) CO_2 utilization obtained with CEM-BL configuration.

the CEM, except at 300 mA cm^{-2}, where it increases from 3.7 to 4 V; way lower to the high 5.3 V bias required with BPM.

Figure 7 illustrates the amount of CO_2 recovered within the CEM-BL BE and the percentage converted into CO_2RR products. At 100 mA cm^{-2}, the flux of regenerated CO_2 is comparable to that of the BPM BE and increases with raising the current density, as expected.[10a] The CO_2 utilization is peaked at 200 mA cm^{-2}, reaching 87%. This carbon efficiency surpasses the typical values reported for alkaline gas-fed CO_2 electrolyzers,[19] confirming once again the promising goodness of the RCCC approach. In an ideal RCCC, the unconverted CO_2 is easily recyclable: the solution exiting the BE tends to be alkaline, enabling it to recapture the unconverted CO_2.[10g] Conversely, the intrinsic characteristics of the GFCC make it significantly more challenging to recycle the large quantities of unconverted CO_2 exiting the alkaline gas-fed electrolyzer.[20] The optimized CEM-BL setup, with a selectivity for formate of ≈55% at 200 mA cm^{-2}, with a cell potential of 3.4 V, and a carbon utilization rate of 87%, is used in the next section to compare the energetic cost of RCCC with respect to GFCC.

2.3. Energy Consumption Assessment

Once the best configuration for a BE producing formate has been found, it is crucial to understand if a RCCC employing this optimized electrolyzer is competitive with a GFCC using a standard gas-fed electrolyzer. To identify the most cost-effective technology, we chose the energy consumption (EC) per mole of product at the end of the carbon chain as the figure of merit (see Supporting Information). The energy costs for the various steps of the carbon chain were obtained from the literature and are summarized in **Table 1**. Unlike GFCC, RCCC eliminates the need for CO_2 recovery and compression, as CO_2 is regenerated in gaseous form directly within the electrolyzer from bicarbonate and subsequently converted. Meanwhile, for the electrolysis step in the BE, we used our previously selected configuration. The electrolysis energy consumption was calculated according to Equation (1).

$$EC = \frac{E_{cell}\ F\ n_e}{FE} \quad (1)$$

Equation (1) E_{cell} is the cell voltage, F is the Faraday constant, n_e is moles of electrons involved in the reaction to produce one mole of formate and FE is the Faradaic Efficiency for formate.

Figure 8 illustrates the total energy required to produce one mole of $HCOO^-$/HCOOH for the entire carbon valorization chain, including both capture and electrochemical conversion, with RCCCs utilizing our BEs in BPM and CEM-BL configurations compared to GFCCs based on gas-fed CO_2RR electrolyzers reported in the literature.[8,21]. Gas-fed electrolyzers considered in the energy consumption assessment are all characterized by a three-chambers configuration fed by a pure stream of CO_2. Notably, at industrial-level current densities (≥200 mA cm^{-2}),[22] the CEM-BL configuration demonstrates lower energy consumption than BPM (Figure 8a). This indicates that, unless new BPM technologies are developed in the near future, CEM configurations are preferable in BEs. It is important to note that, in terms of scalability, both configurations present certain limitations. The use of a BPM enables continuous regeneration of the alkaline anolyte. In contrast, when employing a CEM, the anolyte (i.e., H_2O) serves as a proton source, which can lead to some pH instability. However, as shown in Figure S3b (Supporting Information), the pH variation over time is sufficiently small to be

Table 1. Energetic costs of the capture steps involved in the RCCC and GFCC per mole of CO_2.

	RCCC	GFCC
CO_2 Absorption (kJ mol^{-1})	10[15,25]	13[15,25]
CO_2 Recovery (kJ mol^{-1})	0	178[6,15]
CO_2 Compression (kJ mol^{-1})	0	20[6,15]

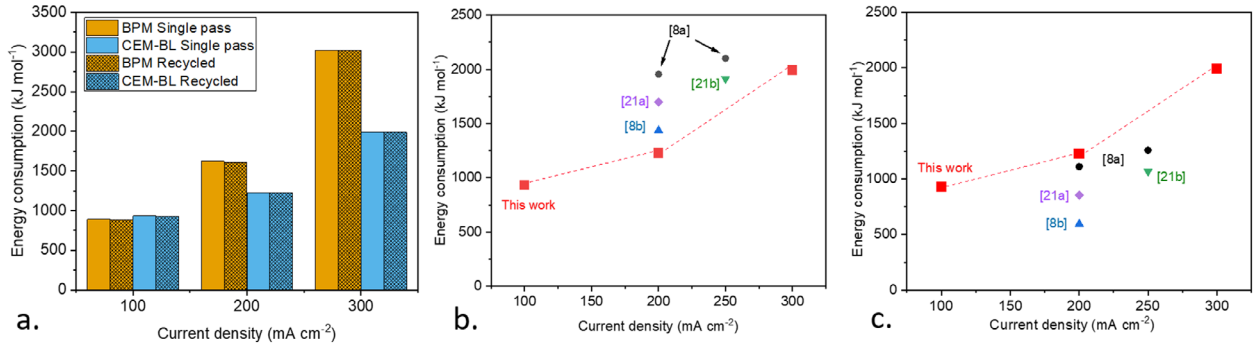

Figure 8. Comparison of EC per mole of final product between RCCC utilizing BPM/CEM-BL based bicarbonate electrolyzers and GFCC employing gas-fed electrolyzers from the literature. a) **RCCC**: comparison of EC of an RCCC using BPM/CEM-BL BEs in single pass and with a CO_2 recycling system b) **Single-pass system**: RCCC and GFCC operate with a single-pass setup where unreacted CO_2 is lost, making the energy consumption of each valorization chain dependent on the CO_2 utilization rate of the CO_2RR electrolyzer. b) **CO_2 recycling**: Unreacted CO_2 at the outlet of RCCC and GFCC is captured and recirculated to the electrolyzer, resulting in 100% CO_2 utilization.

considered a manageable issue. On the other hand, while CEMs are already implemented in commercial systems (e.g., fuel cells and electrolyzers),[23] BPMs remain an emerging technology and are subject to challenges such as delamination during long-term use. Moreover, nowadays BPMs are more expensive than CEMs.[24] Furthermore, the buffer layer plays a critical role when using CEMs. It significantly enhances faradaic efficiencies, thereby reducing the energy cost per mole of formate produced.

However, further investigation is required to fully understand this relatively novel BE component. When CO_2 is used in a single pass (Figure 8b), meaning the unconverted CO_2 exiting the RCCC or GFCC is lost, the RCCC shows lower energy consumption compared to all GFCC systems reported in the literature. In this analysis, the CO_2 utilization for gas-fed electrolyzers is set at 20%, an optimistic average based on literature data.[19] Figure 8c explores a scenario where unconverted CO_2 is recycled, ensuring complete conversion of captured CO_2 into $HCOO^-$/HCOOH. With 100% CO_2 utilization (recycling), GFCCs demonstrate a relatively larger reduction in total energy demand. This is because the energy consumption associated with capture processes has a greater impact on the total energy assessment and is significantly reduced when unreacted CO_2 is recycled.[6b,15,25] On the other hand, recycling CO_2 does not significantly reduce the energy consumption for RCCCs (Figure 8a), since the relative impact of capture process is negligible (Figure S6, Supporting Information). Nevertheless, the RCCC becomes more energy demanding, but it remains competitive. It is also worth noting that implementing a recycling system in a GFCC might be more energetically challenging compared to an RCCC.[15,26] In fact, in alkaline gas-fed electrolyzers, a substantial portion of gaseous CO_2 is lost due to its conversion into (bi)carbonate, necessitating its recovery and reconstitution into gaseous form.[26] Conversely, in BEs, the alkaline solution exiting the electrolyzer can be utilized to recapture the unconverted CO_2, offering a more integrated and energy-efficient solution.[27]

2.4. Anolyte Optimization

When the BE utilizes a CEM instead of a BPM, modifications to the anodic side of the cell become necessary. The anolyte must maintain a sufficient H^+ concentration to ensure proton transport to cathode through the membrane and enable the release of *i*-CO_2.[11] While the proton flux through the membrane is generally governed by the current, a pH gradient between a neutral catholyte and an acidic anolyte can result in proton diffusion toward the catholyte, in addition to the electro-migration phenomenon.[28] To address this issue, we investigated the effect of proton concentration in the anolyte on the BE's performance.

From **Figure 9**, it can be observed that the effect of anolyte concentration, though limited, is indeed present. A 0.05 M H_2SO_4 solution proves to be the optimal anolyte, demonstrating the highest selectivity for formate. At higher concentrations, increased proton diffusion becomes more pronounced, slightly impacting the CO_2RR. The experiments did not reveal any significant impact of the anolyte concentration on cell voltage (Figure S2, Supporting Information). The optimization of the anolyte in the CEM-BL configuration has resulted in higher FEs for formate, lowering the EC of the RCCC. We also demonstrated the stability of the acid anolyte over time, observing only a slight decrease

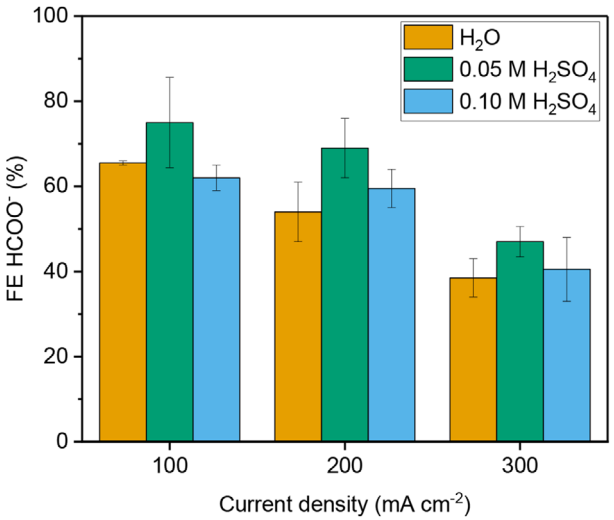

Figure 9. FEs achieved in the CEM-BL configuration under varying proton concentrations in the anolyte.

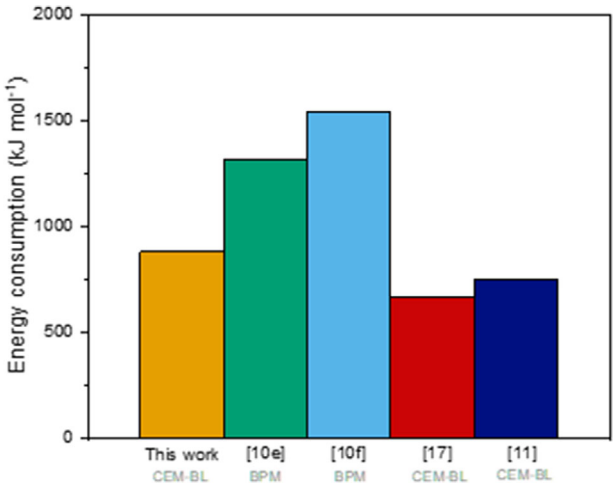

Figure 10. Comparison among energy consumptions due to the electrolysis at 100 mA cm^{-2} in BEs from literature. In this data, a system for CO_2 recycling has been considered (i.e., CO_2 utilization of 100%).

in pH. During this stability test, the FE for formate gradually decreases due to the increasing difficulty in locally recovering CO_2 (Figure S3, Supporting Information). This is caused by a rise in pH over time, as CO_2RR byproducts shift the equilibrium from bicarbonate to carbonate, thereby reducing the system's regeneration capacity.[29]

Figure 10 compares the energy consumption of our BE (CEM-BL with 0.05 M H_2SO_4 as anolyte) with other BEs from literature producing formate.[10e,f,11,17] Best performances have been achieved by using CEM-BL configurations, hence the BE optimized in this work is comparable to the best-performing systems. Also Figure 10 highlights significant potential for further improvements, strengthening the RCCC as a more energy-efficient and practical solution.

3. Conclusion

In this work, a comprehensive study of the BE electrolyzer and its intrinsic mechanisms is conducted, alongside the optimization of the CEM-BL bicarbonate electrolyzer, to demonstrate the competitiveness of the RCCC compared to the GFCC in formate/formic acid electro-production. Our optimized BE operates at 3.4 V and 200 mA cm^{-2}, achieving a formate FE of ≈70%. When no CO_2 recycling is included in the valorization chain, the RCCC demonstrates a clear advantage over the more widely studied GFCC. Even when CO_2 recycling is implemented, the RCCC remains competitive due to the minimal energetic costs associated with its capture steps. It is worth noting that recent gas-fed setups can directly produce formic acid as the final product, unlike BEs, which typically yield formate.[8b] Consequently, if formic acid is the desired end product, the RCCC requires an additional distillation step to convert formate into formic acid.[3a] Given the significant potential for further improvements in BE performance (e.g., reducing cell potential and enhancing FEs), the RCCC stands out as a promising technological approach for converting CO_2 into $HCOO^-$/HCOOH.

Supporting Information

Supporting Information is available from the Wiley Online Library or from the author.

Acknowledgements

J.Z. received the fund under the National Recovery and Resilience Plan (NRRP) – Project code: IR0000027, Concession Decree No. 128 of 21/06/2022 adopted by the Italian Ministry of Research, CUP: B33C22000710006, Project title: iENTRANCE. This study was partially developed in the framework of the research activities carried out within the Project "Network 4 Energy Sustainable Transition—NEST", Spoke 4, Project code PE0000021, funded under the National Recovery and Resilience Plan (NRRP), Mission 4, Component 2, Investment 1.3— Call for tender No. 1561 of 11.10.2022 of Ministero dell'Universita' e della Ricerca (MUR); funded by the European Union—NextGenerationEU. Moreover, it was partially developed with the support of the "Fondazione Compagnia di San Paolo", as part of the VEIColo – Line 1 grant program.

Open access publishing facilitated by Istituto Italiano di Tecnologia, as part of the Wiley - CRUI-CARE agreement.

Conflict of Interest

The authors declare no conflict of interest.

Data Availability Statement

The data that support the findings of this study are available from the corresponding author upon reasonable request.

Keywords

bicarbonate electrolyzer, CO_2 electroreduction, formate electroproduction, reactive carbon capture

Received: January 28, 2025
Revised: April 14, 2025
Published online:

[1] M. Agliuzza, A. Mezza, A. Sacco, *Appl. Energy* **2023**, *334*, 120649.
[2] a) G. Leonzio, A. Hankin, N. Shah, *Chem. Eng. Res. Des.* **2024**, *208*, 934; b) A. Carpignano, R. Gerboni, A. Mezza, C. F. Pirri, A. Sacco, D. Sassone, A. Suriano, A. C. Uggenti, F. Verga, D. Viberti, *J. Mar. Sci. Eng.* **2023**, *11*, 1544.
[3] a) Z. Wang, J. Yan, H. Wang, W. Fu, D. He, B. Wang, Y. Wang, T. Xu, *J. Membr. Sci.* **2024**, *708*, 123016; b) S. Chatterjee, I. Dutta, Y. Lum, Z. Lai, K.-W. Huang, *Energy Environ. Sci.* **2021**, *14*, 1194; c) J. Zeng, N. B. D. Monti, T. Chen, M. Castellino, W. Ju, M. A. O. Lourenço, P. Jagdale, C. F. Pirri, *Catal. Today* **2024**, *437*, 114743.
[4] Q. Ye, X. Zhao, R. Jin, F. Dong, H. Xie, B. Deng, *J. Mater. Chem. A* **2023**, *11*, 21498.
[5] a) J. Disch, L. Bohn, L. Metzler, S. Vierrath, *J. Mater. Chem. A* **2023**, *11*, 7344; b) G. Larrazábal, P. Strøm-Hansen, J. P. Heli, K. Zeiter, K. T. Therkildsen, I. Chorkendorff, B. Seger, *ACS Appl. Mater. Interfaces* **2019**, *11*, 41281.
[6] a) H. Shin, K. U. Hansen, F. Jiao, *Nat. Sustain.* **2021**, *4*, 911; b) D. W. Keith, G. Holmes, D. St Angelo, K. Heidel, *Joule* **2018**, *2*, 1573; c) A. Mezza, A. Pettigiani, N. B. D. Monti, S. Bocchini, M. A. Farkhondehfal, J. Zeng, A. Chiodoni, C. F. Pirri, A. Sacco, *Energies* **2021**, *14*, 7869.

[7] K. Fernández-Caso, G. Díaz-Sainz, M. Alvarez-Guerra, A. Irabien, *ACS Energy Lett.* **2023**, *8*, 1992;
[8] a) H. Yang, J. J. Kaczur, S. D. Sajjad, R. I. Masel, *J. CO2 Util.* **2020**, *42*, 101349; b) L. Fan, C. Xia, P. Zhu, Y. Lu, H. Wang, *Nat. Commun.* **2020**, *11*, 3633.
[9] H. Yang, J. J. Kaczur, S. D. Sajjad, R. I. Masel, *J. CO2 Util.* **2017**, *20*, 208.
[10] a) A. Mezza, M. Bartoli, A. Chiodoni, J. Zeng, C. F. Pirri, A. Sacco, *Nanomaterials* **2023**, *13*, 2314; b) T. Li, E. W. Lees, M. Goldman, D. A. Salvatore, D. M. Weekes, C. P. Berlinguette, *Joule* **2019**, *3*, 1487; c) Y. C. Li, G. Lee, T. Yuan, Y. Wang, D.-H. Nam, Z. Wang, F. P. García de Arquer, Y. Lum, C.-T. Dinh, O. Voznyy, E. H. Sargent, *ACS Energy Lett.* **2019**, *4*, 1427; d) J. Lee, H. Liu, W. Li, *ChemSusChem* **2022**, *15*, 202201329; e) T. Li, E. W. Lees, Z. Zhang, C. P. Berlinguette, *ACS Energy Lett.* **2020**, *5*, 2624; f) O. Gutiérrez-Sánchez, B. de Mot, M. Bulut, D. Pant, T. Breugelmans, *ACS Appl. Mater. Interfaces* **2022**, *14*, 30760; g) Y. Kim, M. Namdari, A. M. L. Jewlal, Y. Chen, D. J. D. Pimlott, M. Stolar, C. P. Berlinguette, *ACS Energy Lett.* **2024**, *10*, 403.
[11] Z. Zhang, D. Xi, Z. Ren, J. Li, *Cell Rep. Phys. Sci.* **2023**, *4*, 101662.
[12] Y. C. Li, Z. Yan, J. Hitt, R. Wycisk, P. N. Pintauro, T. E. Mallouk, *Adv. Sustainable Syst.* **2018**, *2*, 1700187.
[13] M. Namdari, Y. Kim, D. J. D. Pimlott, A. M. L. Jewlal, C. P. Berlinguette, *Chem. Soc. Rev.* **2025**, *54*, 590.
[14] M. A. Blommaert, S. Subramanian, K. Yang, W. A. Smith, D. A. Vermaas, *ACS Appl. Mater. Interfaces* **2021**, *14*, 557.
[15] Z. Zhang, E. W. Lees, S. Ren, B. A. W. Mowbray, A. Huang, C. P. Berlinguette, *ACS Cent. Sci.* **2022**, *8*, 749.
[16] G. Lee, A. S. Rasouli, B.-H. Lee, J. Zhang, D. H. Won, Y. C. Xiao, J. P. Edwards, M. G. Lee, E. D. Jung, F. Arabyarmohammadi, H. Liu, I. Grigioni, J. Abed, T. Alkayyali, S. Liu, K. Xie, R. K. Miao, S. Park, R. Dorakhan, Y. Zhao, C. P. O'Brien, Z. Chen, D. Sinton, E. Sargent, *Joule* **2023**, *7*, 1277.
[17] K. Nomoto, T. Okazaki, K. Beppu, T. Shishido, F. Amano, *EES Catal.* **2024**, *12*, 2357.
[18] T. Kulkarni, B. Yang, X. Zhang, R. Kumar, C. G. Arges, *ACS Appl. Energy Mater.* **2024**, *7*, 11361.
[19] Y. Qiao, W. Lai, K. Huang, T. Yu, Q. Wang, L. Gao, Z. Yang, Z. Ma, T. Sun, M. Liu, C. Lian, H. Huang, *ACS Catal.* **2022**, *12*, 2357.
[20] M. Sassenburg, M. Kelly, S. Subramanian, W. A. Smith, T. Burdyny, *ACS Energy Lett.* **2023**, *8*, 321.
[21] a) L. Hu, J. A. Wrubel, C. M. Baez-Cotto, F. Intia, J. H. Park, A. J. Kropf, N. Kariuki, Z. Huang, A. Farghaly, L. Amichi, P. Saha, L. Tao, D. A. Cullen, D. J. Myers, M. S. Ferrandon, K. C. Neyerlin, *Nat. Commun.* **2023**, *14*, 7605; b) L. Lin, X. He, X.-G. Zhang, W. Ma, B. Zhang, D. Wei, S. Xie, Q. Zhang, X. Yi, Y. Wang, *Angew. Chem., Int. Ed.* **2023**, *62*, 202214959.
[22] B. van den Bosch, J. Krasovic, B. Rawls, A. L. Jongerius, *Current Opinion Green Sustainable Chem.* **2022**, *34*, 100592.
[23] V. Ruuskanen, J. Koponen, K. Huoman, A. Kosonen, M. Niemelä, J. Ahola, *Int. J. Hydrogen Energy* **2017**, *42*, 10775.
[24] Y. Chen, J. A. Wrubel, W. E. Klein, S. Kabir, W. A. Smith, K. C. Neyerlin, T. G. Deutsch, *ACS Appl. Polym. Mater* **2020**, *2*, 4559.
[25] A. J. Welch, E. Dunn, J. S. DuChene, H. A. Atwater, *ACS Energy Lett.* **2020**, *5*, 940.
[26] J. A. Rabinowitz, M. W. Kanan, *Nat. Commun.* **2020**, *11*, 5231.
[27] Y. Kim, E. W. Lees, C. Donde, A. M. L. Jewlal, C. E. B. Waizenegger, B. M. W. De Hepcée, G. L. Simpson, A. Valji, C. P. Berlinguette, *Joule* **2024**, *8*, 3106.
[28] J. Kamcev, R. Sujanani, E.-S. Jang, N. Yan, N. Moe, D. R. Paul, B. D. Freeman, *J. Membr. Sci.* **2018**, *547*, 123.
[29] H. Song, C. A. Fernández, H. Choi, P.-W. Huang, J. Oh, M. C. Hatzell, *Energy Environ. Sci.* **2024**, *17*, 3570.